Műszaki Katonai Közlöny

XXIII. évfolyam, 2013. 2. szám

Róbert NAGY[1], Zsolt ROMÁN[2]

CHANNELLING AND ATTENUATING EFFECTS OF BLAST PARAMETERS IN URBAN STREET GEOMETRY WITH GLAZING[3]

INTRODUCTION

In recent years, a few studies have been carried out to determine formulae describing parameters of explosions taken place in street canyons. This paper quantifies the magnification effect resulting from the multiple reflections of the shock front and the complex interaction of the reflected waves with respect to the street width and façade height. When windows shatter, air leaks through them attenuating the confinement effect that is, decreasing the parameters of the amplified shock wave. A 3D computational fluid dynamics (CFD) aided analysis was carried out for a general street arrangement to capture this phenomenon, and present a modification factor to account for it.

METHODOLOGY

We compare the results of three types of explosion scenarios. The first is a hemispherical surface burst. The other two are explosions in a narrow street canyon, initially without considering the attenuating effect of the windows shattering due to the shock wave, while finally accounting for it. In case of the first arrangement the Kingery-Bulmash empirical formulae are compared to the results of the CFD simulations to validate our model, while in the latter two only the parameterized numerical analyses were carried out concerning different street widths, façade heights and window sizes.

Arrangement

The sketch of the investigated geometry is presented in Figure 1 with the window height parameters and the corresponding glazing surface ratio given in Table 1, while the corresponding street geometry parameters are given in Table 2.

[1] PhD-aspirant of National University of Public Service.
[2] PhD-aspirant of National University of Public Service.
[3] Lectored by: LC. Dr. Zoltán Kovács, associate professor, National University of Public Service.

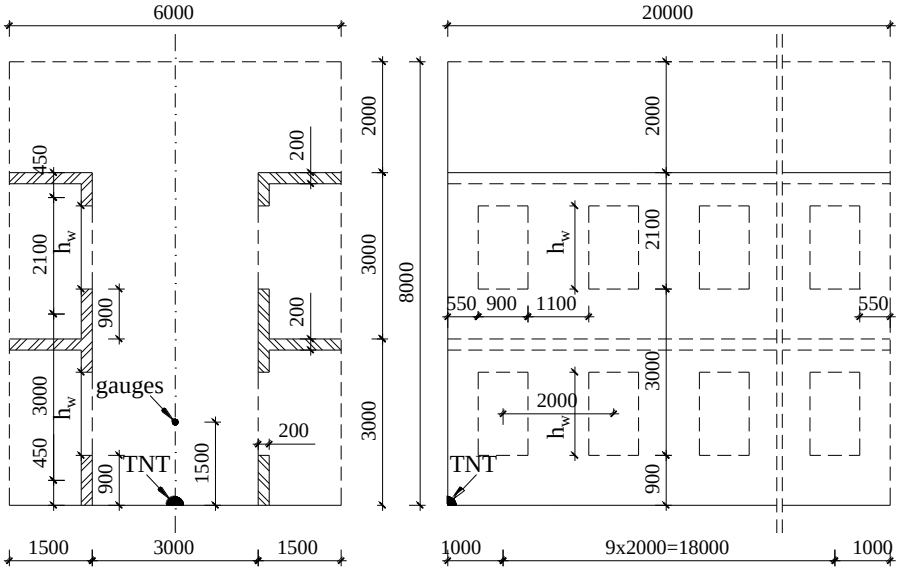

Figure 1. Cross section (left) and side view (right) of the analysed geometry with the dimensions of the model measured in mm.

window width	[m]	0.9										
window height	[m]	0.9	1.0	1.1	1.2	1.3	1.4	1.5	1.6	1.7	1.8	1.9
window area	[m^2]	0.8	0.9	1.0	1.1	1.2	1.3	1.4	1.4	1.5	1.6	1.7
corresp. facade area	[m^2]	6.0										
area ratio	[-]	0.135	0.150	0.165	0.180	0.195	0.210	0.225	0.240	0.255	0.270	0.285

Table 1. Parameters of the window geometry

street width	[m]	2	2.4	2.8	3.2	3.6	4	4.4	4.8	5.2	5.6	6	Charge mass 10kg		
scaled street width	[$m/kg^{1/3}$]	0.93	1.11	1.30	1.49	1.67	1.86	2.04	2.23	2.41	2.60	2.78			
facade height	[m]	1	1.5	2	2.5	3	3.5	4	4.5	5	5.5	6	6.5	7	7.5
scaled facade height	[$m/kg^{1/3}$]	0.46	0.70	0.93	1.16	1.39	1.62	1.86	2.09	2.32	2.55	2.78	3.02	3.25	3.48

Table 2. Parameters of the street geometry

NUMERICAL MODEL

The program

The present study was carried out using the ProSAir explicit hydrocode, developed at Cranfield University [1]. In the program, a spherical symmetric, 1D propellant burning model is implemented, referred to as bulk burn model in the literature [2], where the propellant is assumed to consist of sub-grid sized grains burning on their surfaces. The results of the fully terminated reaction are mapped onto a 2D cylindrical or a 3D Cartesian grid. The shock front propagation is captured by an Advection Upstream Splitting Method (AUSMDV) [7] combined with the MUSCL – Hancock time integration scheme [4] providing second order accuracy both in the time and space domain.

Material parameters

The ambient air is in accordance with the International Standard Metric Conditions (ISMC), having temperature (T0) of 15 °C and pressure (p0) of 101.325 kPa. It is assumed to behave as an ideal gas with molecular degree of freedom (f) of 5 (resulting in the usual specific heat capacity ratio (γ) of 1.4) and average molecular mass (M) of 28.97 g/mol. Consequently the

density (ρ0), the specific internal energy per unit mass (eo) and the specific heat at constant volume (cV) equal to 1.225 kg/m3, 20.68 kJ/kg and 715 J/kg/K respectively.

The high explosive is TNT, in solid state, having density (ρ_{TNT}) of 1600 kg/m^3, detonation velocity (U) of 6730m/s and specific detonation energy per unit mass (E_D) of 4520 kJ/kg. The gaseous detonation products are assumed to have the same properties as air.

The behaviour of the glazing is described by the reflected pressure – reflected impulse iso-damage curve shown in Figure 2. Not aiming at classifying the windows themselves, a simple, common model – irrespective of the width and height of the pane or the properties of the frame – is utilized. The curve is based on experiments of a 7.5 mm thick 1.25 m wide and 1.75 m high laminated window pane with two 3 mm thick glass and a 1.52 mm thick polyvinyl butyral (PVB) interlayer, suitable for blast resistant glazing [3].

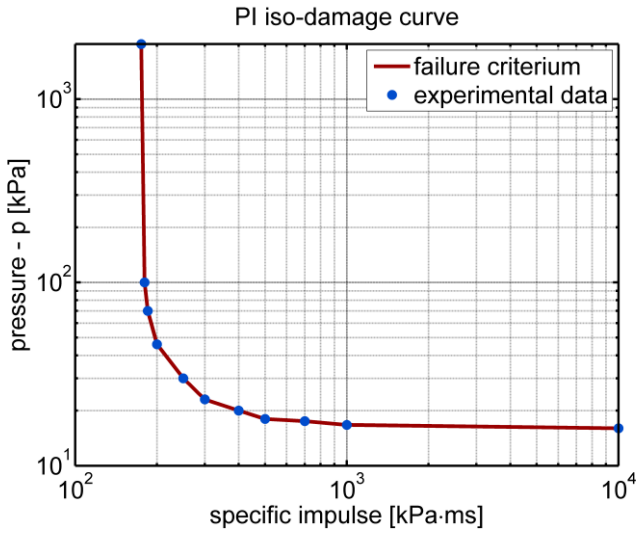

Figure 2. Reflected pressure – reflected impulse iso-damage curve of a 1.25m x 1.75 m x 7.5 mm laminated window pane with PVB interlayer [6].

Geometry

The program allows us to remap calculations of different dimensionality. Exploiting this feature, we always start with the same 1D free air burst. If we accept the assumption of the ground being a perfect reflector without suffering any cratering effect, the hemispherical TNT charge of mass m_{TNT}=10 kg placed on the axis of the street on the ground is possible to be modelled as a spherical propagation of an equivalent spherical charge of mass m_{model}=20 kg. This simulation is valid until the shock front reaches the facade of the buildings situated at least at an $r_{spherical}$=1 m distance from the detonation point.

From that instant, having remapped the field variables to the new model, a 3D simulation is carried out. The arrangement, depicted in Figure 1, has two planes of symmetry; therefore only a quarter of the domain is considered with symmetry boundary conditions (perfect reflective surfaces) at those sides. The model domain is ws=3 m wide, hs=8 m high and ls=20 m long with transmissive boundaries on each side not containing the origin. In case of the rigid façade model, a reflecting obstacle of heights (h) ranging from 1 m to 7.5 m by 0.5 m is positioned at distances from 1 m to 3 m by 0.2 m steps from the street axis yielding street widths (w) of 2 m to 6 m by 0.4 m. In case of the glazing, the street geometry is fixed, where the 6 m high buildings on a 3 m wide street have two stories with windows arranged in a 3 m by 2 m grid on the facade. The width of the windows is always ww=0.9 m in accordance with the most popular dimensions available in Hungary. The height (hw) ranges from 0.9 m to 1.9 m by 0.1 m resulting in glazing ratio (g) from 0.135 to 2.85 by 0.015.

The pressure – time history is extracted at control points on the ground lying in the plane of symmetry of the street in every 10 cm. These data are used to conclude the distinct characteristic injury distances for eardrum and lung damage or lethality [5].

Mesh

The radius of the charge is 144 mm, therefore, by dividing it at least to 50 elements, the optimal cell size is 2.5 mm for the spherical model, consequently having 600 cells in the 1.5 m domain. The 3D model is divided into cubes of 50 mm edge length yielding 3640000cells.

SIMULATION STAGES

Mesh convergence study

In this first step, a 30 m long street channel, with cross similar to the one shown in Figure 1, is investigated. The cell edge lengths are 400 mm, 200 mm, 100 mm, 50mm and 25 mm. The control parameters are the peak positive overpressure and the positive phase impulse measured on the ground along the axis of the street. In Figure 1, the error of the control parameters are depicted as the ratio defined by Equation **Hiba! A hivatkozási forrás nem található.**, where the subscripts *l* and *l/2* refer to the current and the finer (half the edge length) mesh respectively. From Figure 3 we conclude that the model is convergent, and the edge length of 50 mm is sufficient. Half the size results in only approximately 5% increase in accuracy.

$$c_p = \frac{p_{\frac{l}{2}} - p_l}{p_{\frac{l}{2}}}, \quad c_i = \frac{i_{\frac{l}{2}} - i_l}{i_{\frac{l}{2}}} \tag{1}$$

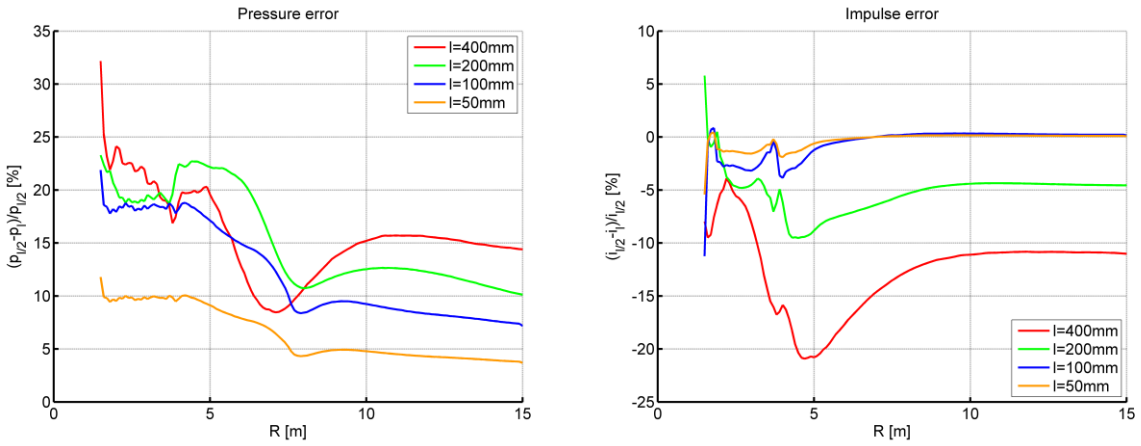

Figure 3. Mesh convergence in case of rigid façade. The peak positive overpressure (left) and the positive phase impulse (right) discrepancies with respect to the values resulting from a mesh of edge length half of the previous measured on the ground along the axis of the street.

Validation

The same 3D geometry as described above – excluding the obstacle – is considered here now with transmissive boundary conditions on the sides and at the top, so we can compare the results of the simulation to the empirical formula by Kingery and Bulmash [8] for hemispherical shock wave properties. The results are in accordance with [9], where the pressure and the impulse error is less than 10% and 25% respectively outside the heat affected zone (scaled dis-

tance approximately 1m/kg$^{1/3}$), which is considered to be acceptable lacking the information on the exact circumstances and the standard deviation of the measurements.

Varying facade height and street width

From the engineering point of view the peak positive overpressure and the positive phase impulse are the two most important values characterizing a blast wave. In the following, we give the dependence of these parameters (measured on ground level, on the street axis) on the façade height, street width, and distance from the detonation point. The charge mass is in every case 10 kg, therefore the scaled distances are easy to determine as well. Figure 4 shows the dependence of the peak positive overpressure and the positive phase impulse on the street width and façade height 5 m away from a 10 kg charge. The multipliers give the ratio of the confined and the free field hemispherical case, and close to the detonation point do not depend on the façade height in the given range. Figure 5 shows, that at greater distances (17 m in this case) with heights increasing the impulse multiplier increases significantly. In Figure 6 and Figure 7 we show the dependence only on the street width at a typical building height (6m). Both parameters show an increase between 200% and 450%, but the confinement effect does not arise until a given distance, indicated in Figure 8. This distance is approximately the width of the street.

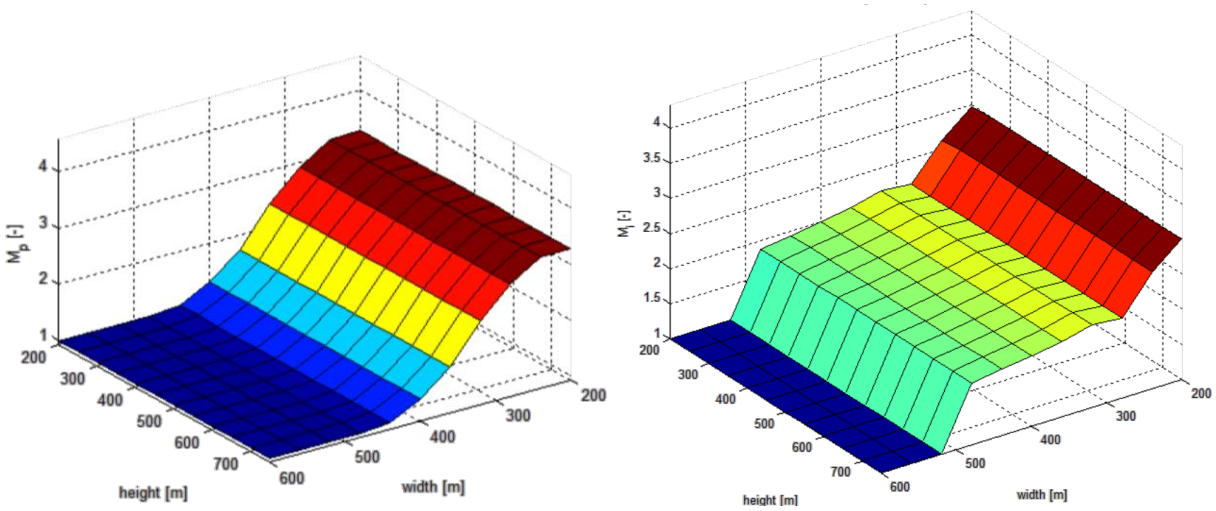

Figure 4. Peak positive overpressure (left) and positive phase impulse (right) multiplier with respect to the street geometry 5 m away from the 10 kg charge

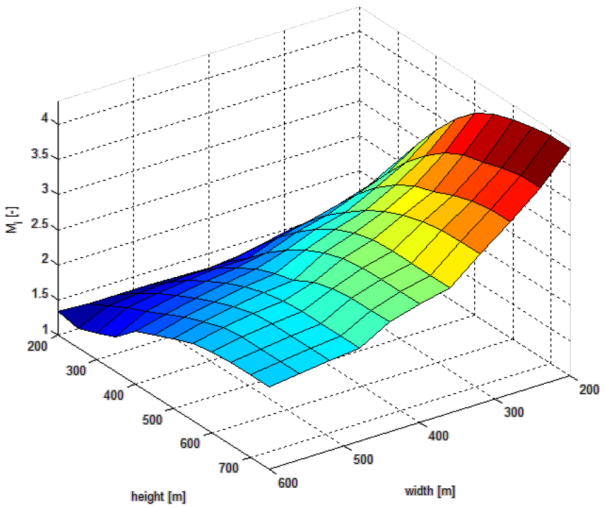

Figure 5. Positive phase impulse multiplier with respect to the street geometry 17 m away from the 10 kg charge

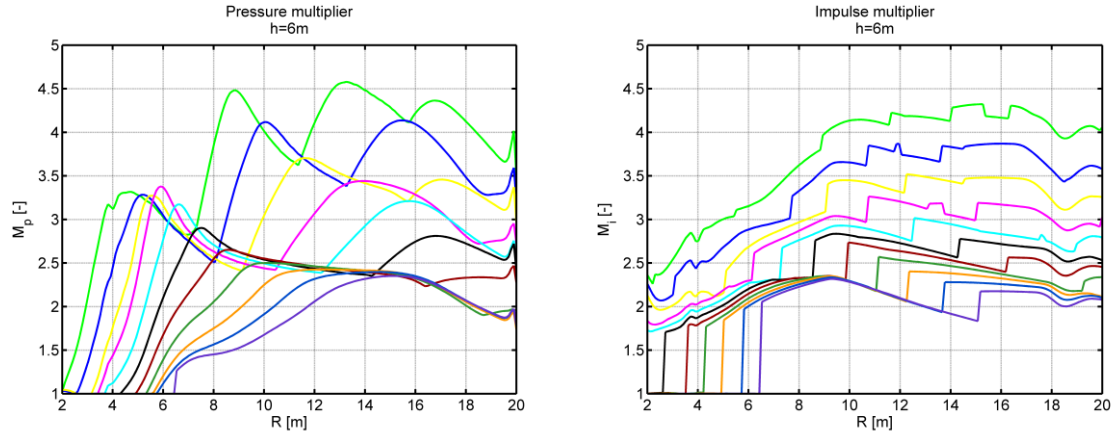

Figure 6. Pressure (left) and impulse (right) multipliers with fixed façade height of 6 m. The colour code of the curves defines the street width and is the same as in Figure 7

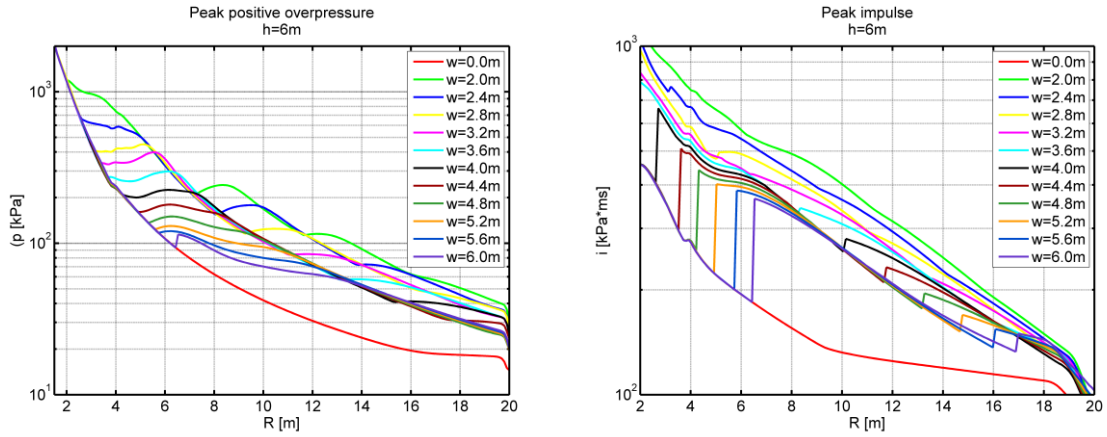

Figure 7. Peak positive overpressure (left) and positive phase impulse (right) with respect to varying street width and fixed façade height of 6 m compared to the free field hemispherical propagation (red curve)

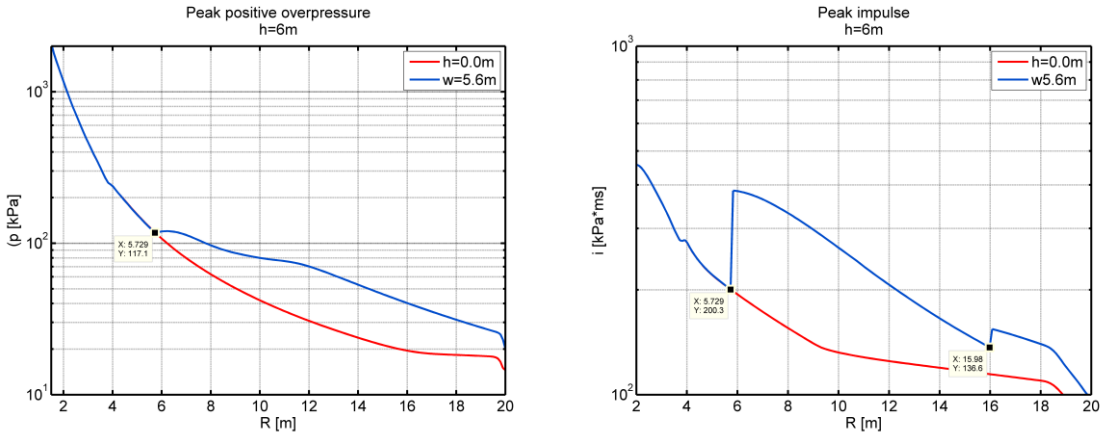

Figure 8. Changes in peak positive overpressure (left) and in positive phase impulse (right) with distance from the detonation point at façade height of 6 m and street width of 5.6 m. Black squares indicate the end of the free field dominated zone.

Having the peak overpressure and the positive phase impulse for each width height, it is possible to determine the stand-off distance for the damage criteria given in [5]. The results are summarized in Figure 10, where the dependence on the height proves to be insignificant, while the dependence on the street width has great effect, as shown by the linear regression:

$$R_{crit} = -3.2017w[m] + 15.635m, \quad if \quad 2m < w < 4m \quad R^2 = 0.9393 \tag{2}$$

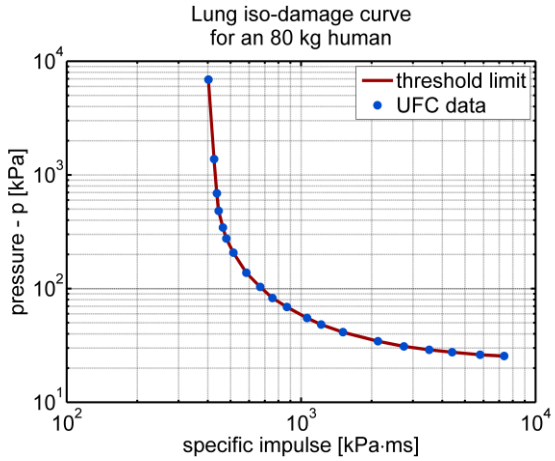

Figure 9. Pressure-impulse iso-damage curve: threshold limit for lung damage of an 80 kg human 46[5]

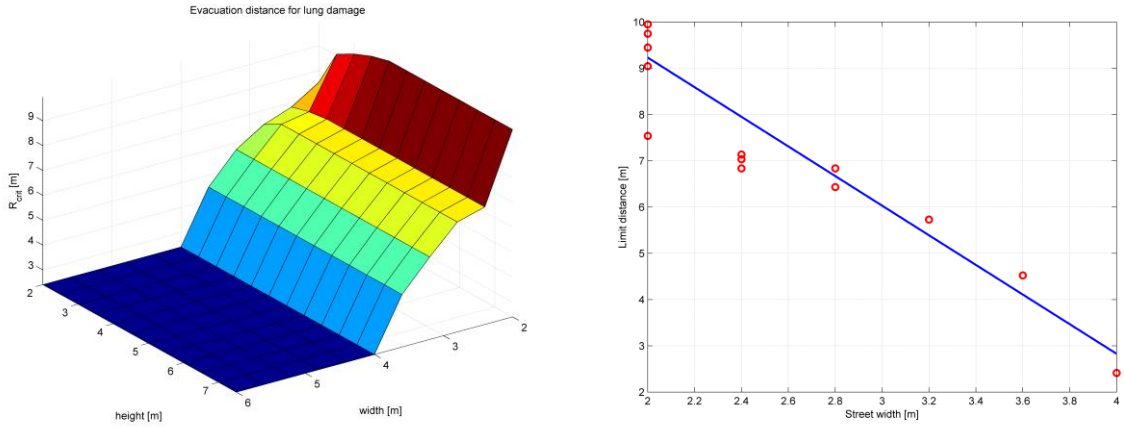

Figure 10. Stand-off distance as a function of the street geometry (left) for lung damage threshold of an 80 kg human. Linear fit for the stand-off distance vs. street width (right)

Varying glazing area ratio

In this section the effect of the glazing is considered. Figure 11 shows, that there is no significant difference in the effect of the different glazing ratios in the range common in Hungary, while it can be concluded that the glazing decreases the pressure and the impulse by approximately 15% and 25% respectively.

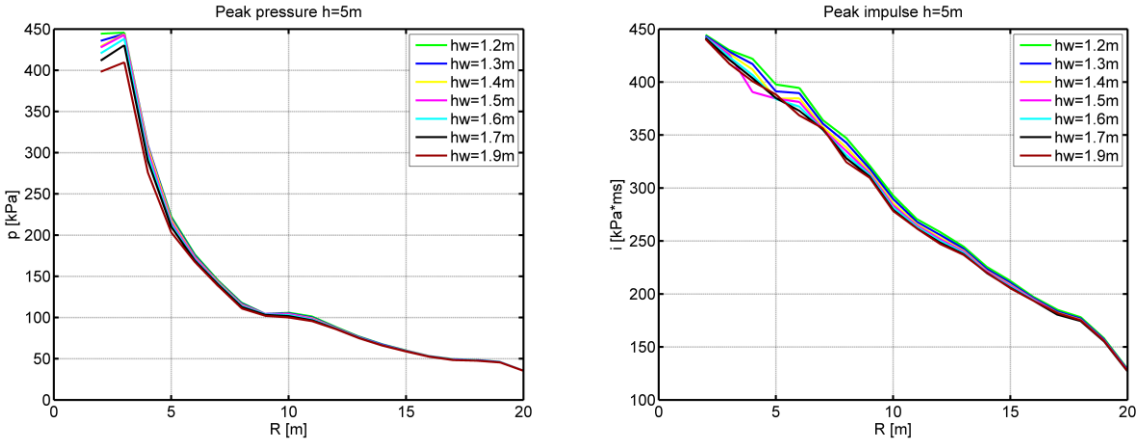

Figure 11. Changes in peak positive overpressure (left) and positive phase impulse (right) due to the increase in the glazing ratio.

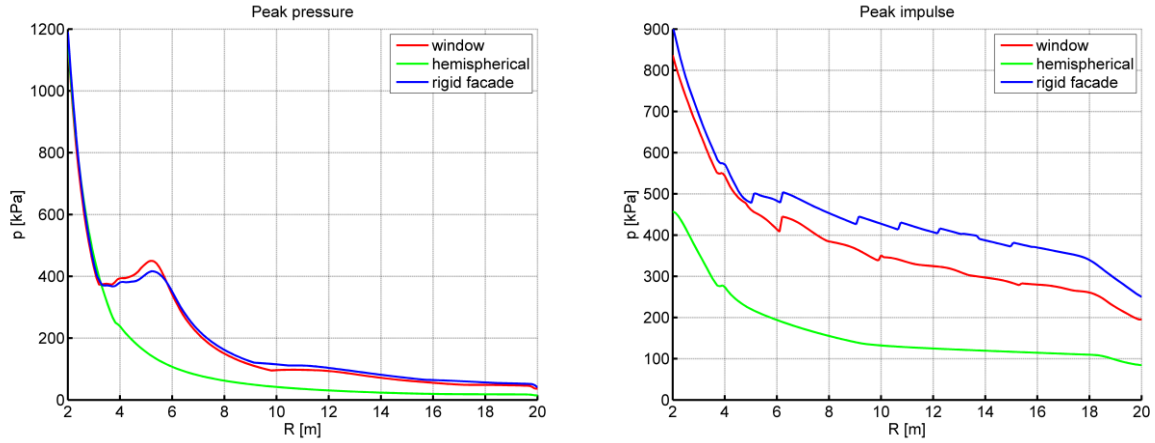

Figure 12. Peak positive overpressure (left) and positive phase impulse (right) in case of free field hemispherical blast wave propagation, rigid wall confinement and façade with glazing

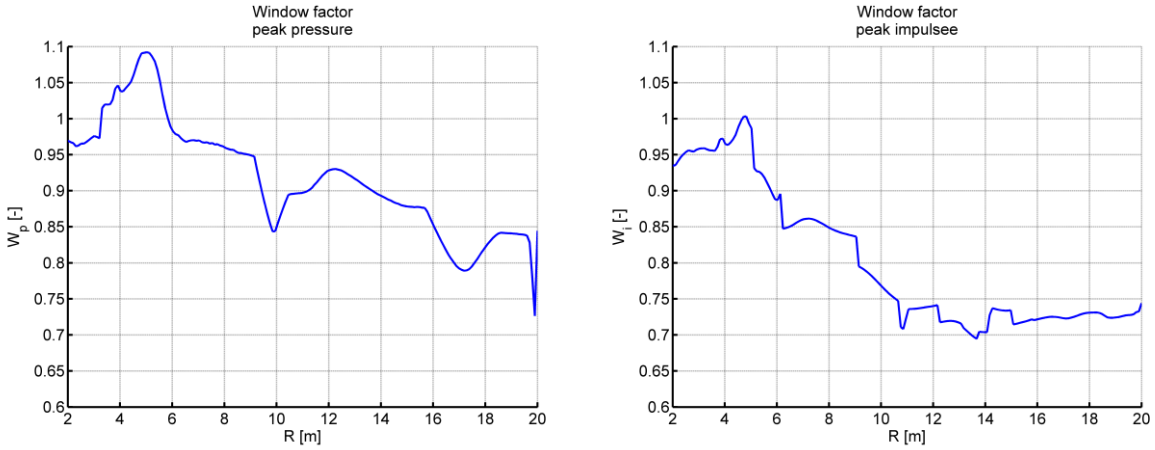

Figure 13. Peak positive overpressure (left) and positive phase impulse (right) correction factors accounting for the attenuating effect of the glazing

CONCLUSION

The complex reflection of the blast waves on tall buildings surrounding narrow street canyons result in magnified parameters of the shock front reaching 4.5 times the values of free-field hemispherical wave. The shattering of the windows decrease them by 15% and 25% for the peak positive overpressure and positive phase impulse respectively.

ACKNOWLEDGEMENT

‘TÁMOP-4.2.1.B-11/2/KMR-2011-0001 The project was realised through the assistance of the European Union, with the co-financing of the European Social Fund.’

REFERENCES

[1] Timothy, A.R., *A computational tool for airblast calculations: Air3d version 9 users’ guide*, User guide, Cranfield University, Engineering Systems Department, Defence College of Management & Technology, Defence Academy of the United Kingdom, Shrivenham, Swindon SN6 8LA, UK, 2006.

[2] Mader, C. L., *Numerical Modelling of Explosives and Propellants*, CRC Press, 3rd edition, 2008, ISBN 978-1-4200-5238-1.
[3] Norville, H. S., and Conrath, E. J., *Considerations for Blast Resistant Glazing Design*, Journal of Architectural Engineering, American Society of Civil Engineers, 7(3):80-86 (2001).
[4] Toro, E. F., *Riemann Solvers and Numerical Methods for Fluid Dynamics, A Practical Introduction*, Springer-Verlag, 1997, ISBN 3- 540-61676-4.
[5] UFC 3-340-02, Structures to Resist the Effects of Accidental Explosions, U.S. Department of Defense, 2008.
[6] Glazing hazard guide: Descriptive tables. Technical report, SAFE/SSG, Explosion Protection, Report No. SSG/EP/1-4/97.
[7] Wada, Y., Liou, M.S., *An accurate and robust flux splitting scheme for shock and contact discontinuities*. Society for Industrial and Applied Mathematics. Journal of Scientific Computing, 18(3):633–657, (1997).
[8] Kingery, C. N.: Air Blast Parameters Versus Scaled Distance For Hemispherical TNT Surface Burst, BRL Report 1344, Sept 1966.
[9] Nagy, R., Román, Zs., *Comparison of empirical and CFD calculated spherical shock wave properties of free air burst*, Blasting Techiques 2013, pp. 312-322 Stara Lesna, ISBN 978-80-970265-5-4.